17th International Coating Science and Technology Symposium
September 7-10, 2014 | Sheraton Carlsbad Resort | San Diego, CA, USA

Reverse Roll Coating at Negative Gaps: Model & Supporting Data

Hadj Benkreira[1], Yusuke Shibata[1, 2] and Katsuya Ito[2]
[1] *Coating Laboratory, University of Bradford, Bradford, UK*
[2]*Films R &D Center, Toyobo Co. Ltd., Otsu, Japan*
Corresponding author:h.benkreira@bradford.ac.uk

EXTENDED ABSTRACT

Keywords: reverse roll coating, negative gap, very thin films, modelling

Introduction: High-tech coating applications (plastic electronics and photo-voltaic for example) are increasingly using roll to roll production for reasons of operation simplicity and costs. In these applications, in order to achieve the required very low film thickness (a few microns), negative gap deformable *forward* roll coating is almost always used. Ribbing instabilities are however inevitable in such a flow and this forces the operation to be conducted at very low speed. The quest for a roll coating method that is stable and can be conducted at high speed to produce very thin films leads us in the present work to consider negative gap deformable *reverse* roll coating. A-priori, this technique may not appear feasible because of the potential of shearing the rubber layer and damaging the substrate but subject to careful start-up we have shown that it works. In previous forums and in a PhD thesis [1], we presented data from a comprehensive experimental programme to demonstrate that very thin stable films can be achieved with this technique making it an inexpensive method to implement in practice (see Figure 1). Here we attempt to underpin our data with a theoretical model.

The Model: The problem at hand is complex as it is an elasto-hydrodynamic flow between two co-rotating rollers, one covered with a rubber sleeve and one rigid roller, the two pressed against each other and forming a negative gap. Using the lubrication approximation, we can write the flow-pressure equation in the thin nip flow as:

$$\frac{dP}{dX} = 12\left[\frac{0.5(1-S)}{H^2} - \frac{Q}{H^3}\right] \qquad (1)$$

with the gap between the rollers given by the geometry of the system as:

$$H = H_{io} + X^2 + \Delta \qquad (2)$$

and the deformation of the roller linked linearly with pressure as:

$$\Delta = Ne^*.P \qquad (3)$$

In these equations, all the quantities are dimensionless expressing fluid pressure $P = p/\frac{\mu v_A}{\bar{r}}$, fluid flow rate $Q = \frac{q}{v_A\bar{r}} \equiv \frac{v_A h_{A,\infty}}{v_A\bar{r}} \equiv \frac{h_{A,\infty}}{\bar{r}} = H_{A,\infty}$, roller speed ratio $S = v_A/v_M$, initial negative gap $H_{io} = h_{io}/\bar{r}$, axial position $X = \frac{x}{\bar{r}}$ and rubber deflection $\Delta = \frac{\delta}{\bar{r}}$ with $\bar{r}\ (= 1/\frac{1}{2}\left(\frac{1}{r_A} + \frac{1}{r_M}\right))$ being defined in the usual manner as the equivalent radius of the applicator and metering rollers, $h_{A,\infty}$ is the film thickness deposited on the applicator roller, the prime quantity of interest in the problem and $Ne^* = \mu v_A/(\frac{2E}{l})\bar{r}^2$ is a modified elasticity number which defines the extent of viscous forces in relation to elastic forces expressed using the elastic modulus *E* of the roll cover and its thickness *l* [2].

At first examination, Eqs (1-3) appear simple to solve if one chooses appropriate boundary conditions. In fact the solution is difficult because of the non-linearity of Eq. (1). In principle this problem does not differ from deformable forward roll coating (see work by Carvalho and Scriven [2,3]) except for the fact that the separation region includes a dynamic wetting line (see figure below) and this complicates the flow analysis. In the presentation, we shall present the model, the predictions derived from it and a comparison with the data measured to underpin the role of the various parameters, H_{io} (initial negative gap), *S* (rollers speeds ratio), Ne^* (modified elasticity number) and Ca_A (applicator roller capillary number) in the control of film thickness.

As just stated, appropriate boundary conditions are required. Here there are two possible sets of conditions.

Case 1: The Reynolds boundary conditions: These state that the flow terminates (at X_m) when both the pressure $P(X_m)$ and pressure drop $dP/dX\ (X_m)$ are zero. From Eqs.(1)-(3), this infers that:

$$\Delta(X_m) = Ne^*.P(X_m) = 0 \qquad (4)$$

$$H(\equiv H_{io} + X_m^2 + \Delta(X_m)) = \frac{Q}{0.5(1-S)} \qquad (5)$$

Thus, for a set speed ratio *S* and gap H_{io}, the following relationship between X_m and Q ($\equiv H_{A,\infty}$) holds:

$$X_m = \left(\frac{Q}{0.5(1-S)} - H_{io}\right)^{1/2} \qquad (6)$$

A unique *Q* can then be find by trial and error, by integrating Eq.(1) from the inlet position assumed far upstream or at $X_i=-1$ with $P(-1)=0$ up to the separation point where a meniscus form X_m until convergence is reached when $P(X_m)= dP/dX\ (X_m) =0$. As Eq. (1) is non-linear, a numerical method of solution is required and this was obtained using the Matlab software with appropriate subroutine to solve stiff non linear differential equation. The predictions from this model will give the film thickness variation with the gap number, H_{io}, a modified elasticity number Ne^*, and the speed ratio *S*. One important observation is that the capillary number plays no part as surface tension effect is not considered in the Reynolds boundary conditions. As a meniscus forms when the flow separates to form a film on the applicator roller, there is no guarantee thus that the X_m found here corresponds to the physical end point of the flow.

Case 2:The capillary pressure boundary condition: This condition allows for the presence of a separation meniscus and balances at the separation meniscus hydrodynamic pressure forces with surface tension forces giving:

$$p(x_m) = -\frac{\sigma}{r_m} \qquad (7a)$$

or using Eq. (7), its dimensionless equivalent

$$P(X_m) = -\frac{\sigma}{r_m}/\mu v_A/\bar{r} \equiv -\frac{1}{R_m Ca_A} \qquad (7b)$$

In this equation, r_m is the radius of curvature of the separation meniscus and R_m is its dimensionless equivalent ($r_m/\bar{r}$). Such condition requires a model of the shape of the meniscus to enable computation of r_m. We use for this the Landau-Levich (1942) and Derjaguin and Levi (1959) or LLD film formation conditions where we liken the profile of the metered film on the applicator roller to that formed in dip coating. In such a situation, the final film thickness, $h_{A,\infty}$ far downstream on the applicator roller and the radius of curvature are simply related, for low capillary number ($Ca_A<<1$) as:

$$h_{A,\infty} = 1.34\, r_m Ca_A^{2/3} \qquad (8)$$

The dimensionless radius of curvature R_m is thus:

$$R_m = H_{A,\infty}/1.34 Ca_A^{2/3} \qquad (9)$$

Substituting this equation into Eq.(7b) enables to define the pressure at the separation meniscus as a function of operating variables and final film thickness or flow rate $H_{A,\infty}$, *i.e.:*

$$P(X_m) = -\frac{1.34\,(Ca_A{}^{-1/3})}{H_{A,\infty}} \qquad (10)$$

We now require the location X_m of the separation meniscus. If we take the similarity with dip coating further, we will observe that the meniscus on the applicator roller side is divisible into two distinct zones, the dynamic meniscus region and the static meniscus region, the two menisci meeting at a stagnation point X_S (not to be confused with X_m). In the static meniscus region, the radius of curvature remains constant. However, in the dynamic meniscus region, from the stagnation point down to the final film thickness on the roller, the film profile continuously changes. On the basis of experimental and theoretical evidence, the film profile can be described by the following exponential form:

$$h_A(x) = h_{A,\infty}[1 + C_1 \exp\left(-\frac{(3Ca_A)^{1/3}x}{h_{A,\infty}}\right)] \qquad (11)$$

or its dimensionless equivalent

$$H_A(x) = H_{A,\infty}[1 + C_1 \exp\left(-\frac{(3Ca_A)^{1/3}X}{H_{A,\infty}}\right)] \qquad (12)$$

C_1 in the above equation is a constant found by fitting the equation to the film thickness data. At the stagnation point, this equation enables the calculation of the dimensionless radius of curvature R_m as follows:

$$\frac{1}{R_m} = \left.\frac{d^2H_A(X)}{dX}\right|_{X_S} = (3Ca)^{2/3}\left(\frac{H_A(X_S)-H_{A,\infty}}{H_{A,\infty}^2}\right) \qquad (13)$$

Substituting Eq.(13) for R_m into the above equation gives the dimensionless thickness $H_A(X_s)$ of the film at the separation point as a simple proportion of the dimensionless final film thickness $H_{A,\infty}$:

$$H_A(X_s) = 1.644 H_{A,\infty} \qquad (14)$$

The corresponding angular position $\theta_{A,m}$ is obtained from the geometry of the system as (see Carvalho and Scriven (1997)):

$$\theta_{A,m} = arctan\{-0.644(3Ca_A)^{1/3}\} \qquad (15)$$

Now to complete the location x_m of the meniscus, we allow the static meniscus to continue with its constant r_m (i.e. as a circle) all the way to the incoming dry metering roller with which it intersects and forms a contact angle, $\theta_{M,c}$, a-priori unknow but which can be fixed from experimental data. The coating gap at the meniscus point is thus given, in dimensionless form as:

$$H(X_m) = 1.644H_{A,\infty} + R_m(cos\theta_{A,m} + cos\theta_{M,c}) \qquad (16)$$

Substituting R_m from Eq. (9) and $\theta_{A,m}$ from Eq. (15) into the above equation will define the separation gap at the meniscus position uniquely as a function of operating variables, contact angle $\theta_{M,c}$ and final film thickness $H_{A,\infty}$.

We can now invoke Eq.(2) and apply it at the meniscus position to fix X_m as a unique function of $H_{A,\infty}$ and operating variables:

$$(X_m) = \left[1.644H_{A,\infty} + \left(H_{A,\infty}/1.34{Ca_A}^{2/3}\right)\left(\cos\left(arctan\left\{-0.644(3Ca_A)^{\frac{1}{3}}\right\}\right) + cos\theta_{M,c}\right) - H_{io} + \frac{1.34\,({Ca_A}^{-1/3})}{H_{A,\infty}}Ne^*\right]^{1/2} \qquad (17)$$

The model is now closed and the solution of these equations can proceed using the following iterative procedure:

(i) Fix operating parameters Ne^*, Ca_A, H_{io}, S and $\theta_{M,c}$

(ii) Guess a value of $H_{A,\infty}$ *(≡Q)*, then calculate R_m , $P(X_m)$, $H_A(X_s)$, $\theta_{A,m}$, $H(X_m)$ and finally X_m using Eqs. (9), (10), (14), (15), (16) and (17) respectively.

(iii) Integrate Eq.(1), beginning at $X_i=-1$ with $P(-1)=0$ and terminating at X_m with a calculated $P(X_m)$.

(iv) Check for convergence that this calculated $P(X_m)= \left[-\frac{1}{R_m Ca_A}\right] = -1.34Ca_A^{-1/3}/H_{A,\infty}$

(v) Alternatively the integration can be carried out backward starting at X_m with $P(X_m)= \left[-\frac{1}{R_m Ca_A}\right] = -1.34Ca_A^{-1/3}/H_{A,\infty}$ and checking that convergence is reached when $P(-1)=0$.

Because of the non-linearity of Eq. (1), a numerical integration is again required. This was performed using Matlab software as with the appropriate integration subroutine.

Results & Discussion: In the presentation, the predictions from this model will be presented, discussed and compared with experimental data (see Figure 3 for typical data) to arrive at a conclusion whether or not such simple modelling is able to capture the essential operation of this flow.

References

1. Y. Shibata, PhD Thesis: High Speed very thin films with reverse roll coating, University of Bradford (UK), 2012
2. M.S. Carvalho and L.E. Scriven, *J. of Computational Physics* **138,** 449–479 (1997)
3. M.S. Carvlho and L.E. Scriven, *J. of Fluid Mech.* 339, 143-172 (1997).

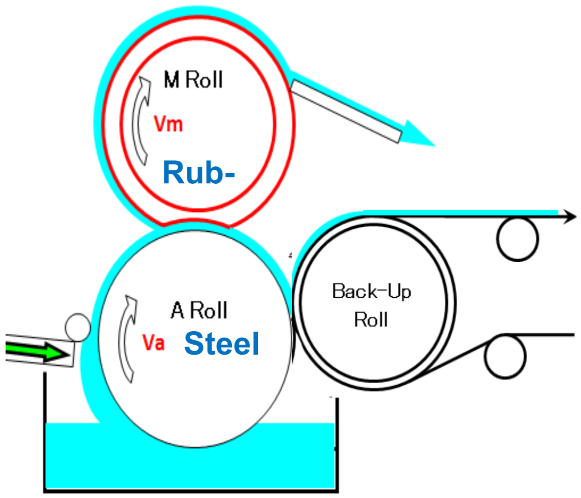

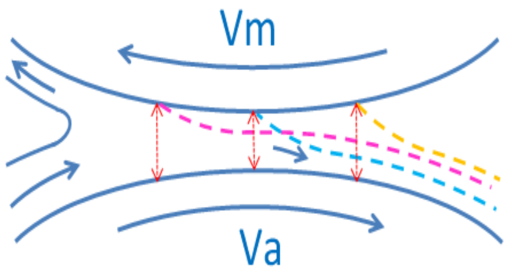

Figure 1: Negative Gap Reverse Roll Coating

Figure 2: Reverse Roll Coating showing dynamic wetting line pinning at different positions. (Although not shown here the metering roller is its deformed position and the coating gap is negative).

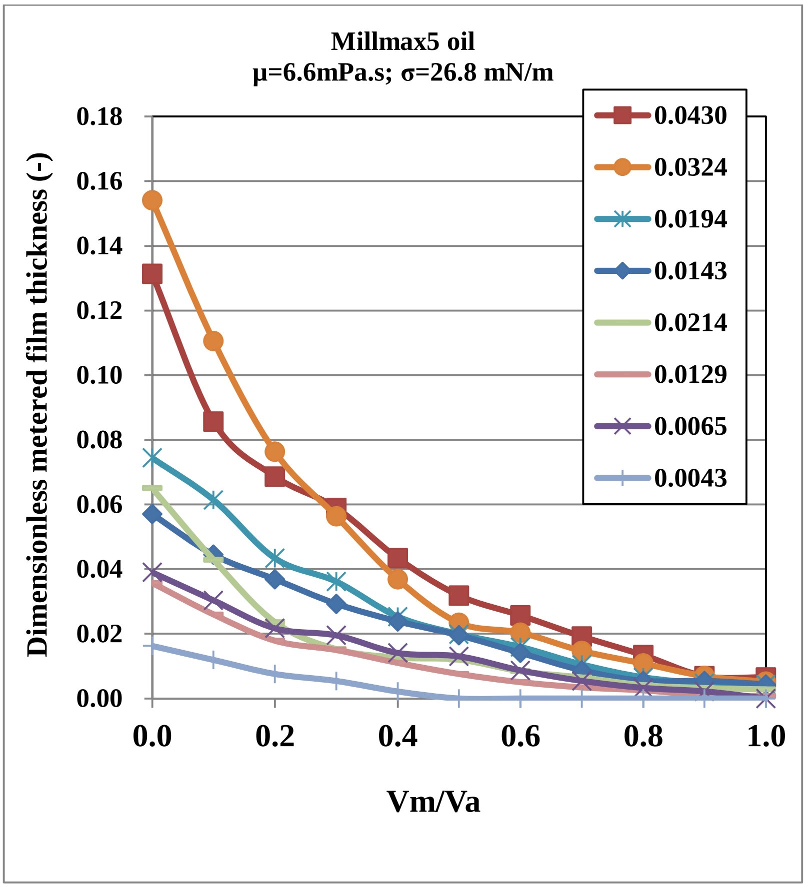

Figure 3: Experimental Data. Here dimensionless thickness is actual thickness divided by – negative gap plotted as a function of speed ratio and for a range of Elasticity Number, $Es = \mu v_A / (\frac{E}{hio})$.